J. Fluid Mech. (1969), *vol.* 38, *part* 3, *pp.* 457–472
Printed in Great Britain

Non-axisymmetric turbulent mass transfer in a circular tube

By ALAN QUARMBY
The University of Manchester Institute of Science and Technology
AND R. K. ANAND
Indian Institute of Technology, Delhi

(Received 27 July 1968)

Theory and experiment are presented for mass transfer into a fully developed turbulent flow in a plain circular tube in two non-axisymmetric cases. The cases studied are a diametral line source and a discontinuous ring source, in which there is a uniform mass flux over rectangular areas of the tube wall. A comparison is made between the concentration profiles predicted by the solutions of the diffusion equation and experiments using nitrous oxide, Schmidt number $S = 0{\cdot}77$, as a tracer gas in air. The range of experiments covers Reynolds numbers R from 20,000 to 120,000.

In the analysis, the assumption is made that the tangential and radial eddy diffusivities of mass are equal at a point. The radial diffusivity of mass, which is a function of radial position, is related to the radial eddy diffusivity of momentum by a ratio, which takes account of fluid properties and the value of the radial eddy diffusivity of momentum. The satisfactory agreement between analysis and experiment establishes the correctness of this assumption. Further confirmation was obtained by direct evaluation of the tangential eddy diffusivity of mass from the measured concentration profiles.

1. Introduction

The non-axisymmetric problem with heat or mass transfer in a tube has received much less attention than the axisymmetric problem. The solution of the non-axisymmetric problem would require a knowledge of the diffusion process in the tangential direction as well as in the radial direction. That is, it is necessary to know the tangential eddy diffusivity of heat $\epsilon_{h,\omega}$ or of mass $\epsilon_{d,\omega}$, as well as the radial diffusivities $\epsilon_{h,r}$ and $\epsilon_{d,r}$. In the axisymmetric situation, much effort has gone into obtaining an acceptable description of the radial eddy diffusivity of heat or mass from the description of the radial eddy diffusivity of momentum $\epsilon_{m,r}$, by use of a suitable expression for their ratio. In the non-axisymmetric case, a logical consequence of this approach is to relate the tangential eddy diffusivity to the radial eddy diffusivity. Such an approach was used by Reynolds (1963) and Sparrow & Lin (1963), who considered heat transfer to a fully developed turbulent flow in a plain tube, which has circumferential variations of wall heat flux or temperature. Sparrow & Black (1967) have given experimental results for

fully developed heat transfer to air in an electrically heated tube, whose varying wall thickness gave a circumferentially varying wall heat flux. Both Reynolds and Sparrow & Lin assumed that $\epsilon_{h,\omega}$ was equal to $\epsilon_{h,r}$ at the same point. However, the temperature profiles predicted by the analysis of Sparrow & Lin agreed with the experiments of Sparrow & Black, only if it was assumed that in the sublayer the ratio of these two quantities was about ten.

A number of criticisms may be made of this work. Thus, an exact solution of the energy equation was not given. The theoretical work was carried out by fitting polynomials and extrapolation of the results. Also, the expression chosen to describe the radial eddy diffusivity gives a value of -1 at the centre of the tube. This is a most unacceptable result, when considering a non-axisymmetric situation, in which heat is transferred across this region. No evidence was presented to establish the correctness of the heat fluxes, and it is not possible to check on the method of calculation of heat flux. Also, Hanold (1967) suggests that some part of the discrepancy between theory and experiment can be attributed to the effect of natural convection, which was not considered in the analysis. Hall & Hashimi (1964) gave an approximate solution of the diffusion equation for mass transfer into a fully developed turbulent flow in a tube from a patch source in the tube wall. This solution neglected tangential diffusivity. It was compared with experimental measurements of the concentration of nitrous oxide made along the axis of the tube wall. The agreement with theory was not good.

It is clear from the above that previous work on the problem of non-axisymmetric heat and mass transfer has not established a description of the tangential eddy diffusivity, or what ratio it has to the radial eddy diffusivity. In the first part of this work, Quarmby & Anand (1969) established results for axisymmetrical mass transfer, which provide a basis from which the non-axisymmetric problem may be considered. The results establish acceptable and accurate descriptions of the velocity profile and of the radial eddy diffusivities of mass and momentum. The experimental apparatus was easily adapted to provide precisely defined non-axisymmetric boundary conditions. Information about the tangential eddy diffusivity and its relation to the radial eddy diffusivity may be obtained in two ways. A solution of the governing equation could be obtained, in which some assumption is made about the ratio of $\epsilon_{d,\omega}$ to $\epsilon_{d,r}$ and the predicted non-axisymmetric concentration profiles compared with the measurements of a complementary experiment. Alternatively, detailed measurements of the non-axisymmetric concentration profiles could be used to calculate the values of tangential eddy diffusivity by a suitable numerical integration scheme. Both these methods were used here.

2. Analysis and formulation of the equations

(i) *The diffusion equation*

Solutions were sought of the diffusion equation in two non-axisymmetric cases. These were: (*a*) a diametral line source, and (*b*) a discontinuous ring source in the tube wall, in which there was a uniform mass flux over only a part of the cylindrical surface.

Like the axisymmetric situations studied in the first part of this work, the two cases were chosen on the ground that, in the first, the diffusion process takes place mainly in the turbulent core, whereas, in the second, it is initially through the sublayer.

For steady-state conditions and constant fluid properties, and neglecting axial diffusion, the concentration c at any point r, x, ω is given by the governing equation

$$u\frac{\partial c}{\partial x} = \frac{1}{r}\frac{\partial}{\partial r}\left[r(D+\epsilon_{d,r})\frac{\partial c}{\partial r}\right] + \frac{1}{r^2}\frac{\partial}{\partial \omega}\left[(D+\epsilon_{d,\omega})\frac{\partial c}{\partial \omega}\right], \tag{1}$$

where u is the velocity of the fluid, density ρ, and D the molecular diffusivity. The non-dimensional variables

$$x^+ = \frac{x}{r_0}, \quad r^+ = \frac{r}{\nu}\left(\frac{\tau_0}{\rho}\right)^{\frac{1}{2}}, \quad u^+ = u\Big/\left(\frac{\tau_0}{\rho}\right)^{\frac{1}{2}} \quad \text{and} \quad \theta = \frac{c}{c_m}$$

are introduced, where τ_0 is the shear stress at the wall of the tube, radius r_0, and ν is the kinematic viscosity.

The bulk mean concentration c_m is defined by

$$c_m = \int_0^{r_0} cur\,dr \Big/ \int_0^{r_0} ur\,dr. \tag{2}$$

Equation (1) becomes

$$u^+\frac{\partial \theta}{dx^+} = \frac{r_0^+}{r^+}\frac{\partial}{\partial r^+}\left[r^+\left(\frac{1}{S}+\frac{\epsilon_{d,r}}{\nu}\right)\frac{\partial \theta}{\partial r^+}\right] + \frac{r_0^+}{r^{+2}}\frac{\partial}{\partial \omega}\left[\left(\frac{1}{S}+\frac{\epsilon_{d\,\omega}}{\nu}\right)\frac{\partial \theta}{\partial \omega}\right], \tag{3a}$$

and the boundary condition on (3a) is

$$\partial\theta/\partial r^+ = 0 \quad \text{at} \quad r^+ = 0 \quad \text{and} \quad r^+ = r_0^+ \quad \text{for all} \quad x^+. \tag{3b}$$

(ii) *The initial profile*

The boundary condition at $x^+ = 0$ is determined experimentally as

$$\theta(0, r^+, \omega) = \theta_i. \tag{4}$$

For non-axisymmetric diffusion, θ_i is a function of r and ω. Since the fully developed concentration profile is uniform for large x^+, as a result of (3b), it is convenient to express θ_i by

$$\theta_i = 1 + A_0 + \sum_{n=1}^{n=\infty} A_n \cos(n\omega'), \tag{5a}$$

where

$$A_n = \sum_{m=0}^{m=6} a_{nm} z^m \tag{5b}$$

and z is r/r_0.

Thus, the initial profile contains the fully developed uniform profile explicitly together with a symmetric A_0, which is a function of radius only, and the functions which include the tangential variation of θ_i. This tangential variation of θ_i is expressed in terms of the angle ω'. The change of angle is made since, if the measured profile is expanded in terms of a Fourier series, the period must be 2π. In the actual cases considered, it will be noted from figures 1 and 2 that the period

of the line source will be π, and that that of the discontinuous ring source will be $\frac{1}{2}\pi$. Such a set up is convenient in the experimental situation, because it allows detailed and extensive measurement to be confined to either one-half or one-quarter of the tube cross-section.

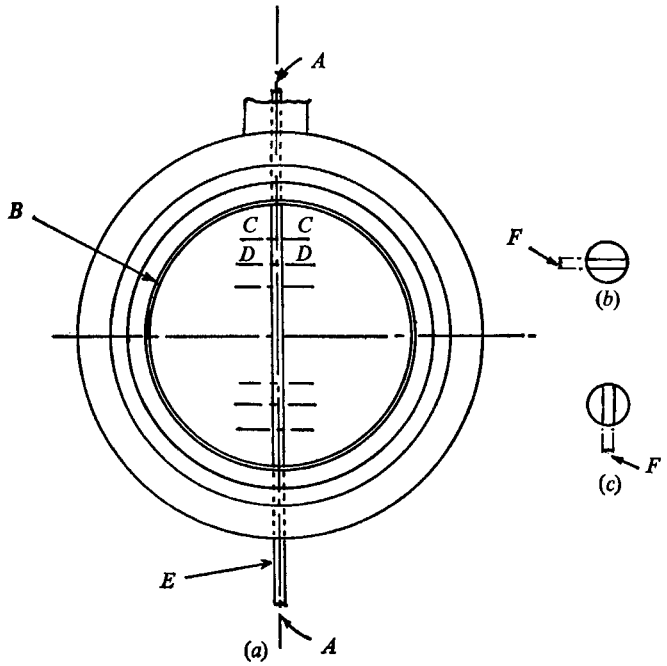

FIGURE 1. Detail of diametrical line source. (*a*) *A*, Nitrous oxide inlet; *B*, brass tube; *E*, stainless-steel hypodermic. (*b*) Section *C–C*. (*c*) Section *D–D*. *F*, 0·010 in.

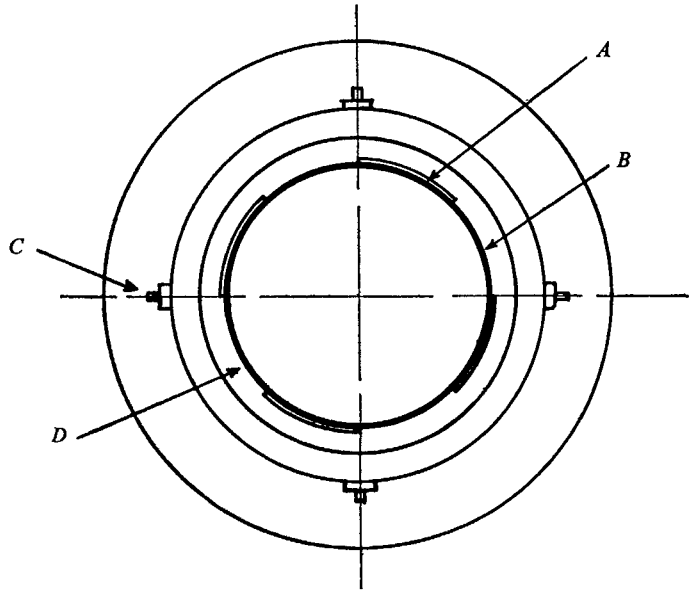

FIGURE 2. Detail of discontinuous ring source. *A*, Impermeable sector; *B*, permeable sector. *C*, nitrous oxide inlet; *D*, Vyon porous plastic.

Thus, for the line source, detailed measurements are made for $0 < \omega < \pi$, and these are expressed in a Fourier series in $\omega' = 2\omega$. Since the function in ω' has zero slope at $\omega' = 0$ and 2π, it follows that a Fourier cosine series will result with the eigenvalues being the integers $1, 2, 3 \ldots$ as given in equation $(5a)$. For the discontinuous ring source $\omega' = 4\omega$, but the Fourier cosine series still holds. In general, the relation between ω and ω' is $\omega' = m\omega$, where m is the periodicity of the initial profile in ω.

(iii) *Solution of the diffusion equation*

The solution is divided into a fully developed part θ_1 and a developing part θ_2. As stated, θ_1 has a uniform value; thus

$$\theta_1 = 1, \tag{6}$$

whilst θ_2 has a symmetric part θ_2' and an unsymmetric part θ_2''. From equation $(5a)$, it follows that the value of θ_2' at $x^+ = 0$ is A_0, whilst

$$\theta_2'' = \sum_{n=1}^{n=\infty} A_n \cos(mn\omega). \tag{7}$$

It is clear that the mixed mean concentration due to θ_2 is zero.

Since θ_1 takes complete account of the fully developed situation, there can be no further addition to it rising from either A_0 or any of the other harmonics. Thus the profile resulting from A_0 will consist only of a decaying axisymmetric profile. The solution for the symmetric diffusion is identical to that given by Quarmby & Anand, and we may write

$$\theta_2' = \sum_{n=1}^{n=\infty} C_n \phi_n \exp\left(-\frac{2\beta_n^2 x^+}{R}\right), \tag{8a}$$

where ϕ_n and β_n are the eigenfunctions and eigenvalues, and the constants C_n are given by

$$C_n = \frac{\int_0^{r_0^+} -A_0 \phi_n u^+ r^+ dr^+}{\int_0^{r_0^+} \phi_n^2 u^+ r^+ dr^+}. \tag{8b}$$

The equation for θ_2'' is

$$u^+ \frac{\partial \theta_2''}{\partial x^+} = \frac{r_0^+}{r^+} \frac{\partial}{\partial r^+}\left[r^+ \left(\frac{1}{S} + \frac{\epsilon_{d,r}}{\nu}\right) \frac{\partial \theta_2''}{\partial r^+}\right] + \frac{r_0^+}{r^{+2}} \frac{\partial}{\partial \omega}\left[\left(\frac{1}{S} + \frac{\epsilon_{d,\omega}}{\nu}\right) \frac{\partial \theta_2''}{\partial \omega}\right], \tag{9}$$

and a variable separable solution is sought to the form

$$\theta_2'' = \psi(x^+) \mathscr{R}(r^+) f(\omega). \tag{10}$$

On re-arrangement we have:

$$\frac{1}{\psi} \frac{\partial \psi}{\partial x^+} = \frac{r_0^+}{u^+ r^+ \mathscr{R}} \frac{\partial}{\partial r^+}\left[r^+ \frac{1}{S} + \frac{\epsilon_{d,r}}{\nu} \frac{\partial \mathscr{R}}{\partial r^+}\right] + \frac{r_0^+}{u^+ r^{+2} f} \frac{\partial}{\partial \omega}\left[\left(\frac{1}{S} + \frac{\epsilon_{d,\omega}}{\nu}\right) \frac{\partial f}{\partial \omega}\right], \tag{11}$$

which may be equated to a constant, $-2a^2/R$.

The solution for ψ is $$\psi(x^+) = \exp\left(-\frac{2\alpha^2}{R}x^+\right), \tag{12}$$

whilst $$\frac{1}{\mathscr{R}}\frac{r_0^+}{r^+}\frac{\partial}{\partial r^+}\left[r^+\left(\frac{1}{S}+\frac{\epsilon_{d,r}}{\nu}\right)\frac{\partial \mathscr{R}}{\partial r^+}\right]+\frac{2\alpha^2 u^+}{R} = -\frac{r_0^+}{r^{+2}}\frac{1}{f}\frac{\partial}{\partial \omega}\left[\left(\frac{1}{S}+\frac{\epsilon_{d,\omega}}{\nu}\right)\frac{\partial f}{\partial \omega}\right]. \tag{13}$$

Since the flow is fully developed and unidirectional, $\epsilon_{d,\omega}$ must be independent of ω and only a function of r^+. We write

$$\frac{1}{S}+\frac{\epsilon_{d,r}}{\nu} = E_r, \tag{14a}$$

and

$$\frac{1}{S}+\frac{\epsilon_{d,\omega}}{\nu} = E_\omega; \tag{14b}$$

and E_ω may be taken out of the right-hand bracket of (13).

Although this is a considerable simplification, a description of E_ω is needed before the solution can proceed. Substituting (14) into (13), and equating to a constant λ^2, we obtain

$$\frac{r^+}{\mathscr{R}E_\omega}\frac{\partial}{\partial r^+}\left[r^+E_r\frac{\partial \mathscr{R}}{\partial r^+}\right]+\frac{2\alpha^2}{R}\frac{u^+r^{+2}}{r_0^+E_\omega} = -\frac{1}{f}\frac{\partial^2 f}{\partial \omega^2} = \lambda^2. \tag{15}$$

The solution for f is

$$f = \sum_{\lambda=0}^{\lambda=\infty} A'_\lambda \cos(\lambda\omega) + B'_\lambda \sin(\lambda\omega). \tag{16}$$

In order to obtain a more general solution of (16), we apply only the condition that at some angle, $\omega = 0$, the tangential profile has zero slope. Since the bulk concentration of θ_2'' has zero value, this condition must hold whatever the circumferential variation of the diffusion source. Accordingly, the solution of (16) is a cosine series, and λ_n are the integers 0, 1, 2, 3, ... It is preferable to use this result for $f(\omega)$, rather than a more restricted form (e.g. $\lambda = 2, 4, 6, \ldots$), since the eigenfunctions $\mathscr{R}$ are determined by the values assigned to λ. Thus, we seek a more general solution of $f(\omega)$, rather than restrict it to the forms of particular initial profile, with which we are concerned in the present case. Also, since the eigenvalue $\lambda = 0$ corresponds to a part of the solution, which is not a function of ω, this eigenvalue is ignored, because all the axisymmetric part of the solution has been accounted for in (8*a*).

Accordingly,

$$f(\omega) = \sum_{\lambda=1}^{\lambda=\infty} A'_\lambda \cos(\lambda\omega), \tag{17}$$

where $\lambda = 1, 2, 3, \ldots$.

The coefficients A'_λ are determined as follows. At $r^+ = r_0^+$ we may normalize the functions $\mathscr{R}(r^+)$. This is permissible since the constants of these eigenfunctions are still to be determined. The initial value is given by (7), so that, at $x^+ = 0$ and $r^+ = r_0^+$,

$$\sum_{\lambda=1}^{\lambda=\infty} A'_\lambda \cos(\lambda\omega) = \sum_{n=1}^{n=\infty} A_n(1)\cos n\omega'. \tag{18}$$

Since each side of (18) is a Fourier cosine series in the same interval, 0–2π, the coefficients must be identical. Thus,

$$\begin{aligned} A'_\lambda &= A_n(1), \\ &= a_{n0} + a_{n1}(1) + a_{n2}(1)^2 \ldots. \end{aligned} \tag{19}$$

That is, the coefficients of $f(\omega)$ are shown to be the sum of the coefficients of the polynomials in r^+ which were fitted to the initial profile.

The solution for $\mathscr{R}(r^+)$ is given by

$$\frac{\partial}{\partial r^+}\left[r^+E_r\frac{\partial \mathscr{R}}{\partial r^+}\right]+\left[\frac{2\alpha^2u^+r^+}{Rr_0^+}-\frac{\lambda^2E_\omega}{r^+}\right]\mathscr{R}=0 \tag{20}$$

with the boundary conditions

$$\frac{\partial \mathscr{R}}{\partial r^+}=0 \quad \text{at} \quad r^+=r_0^+, \tag{21a}$$

since the boundary is impermeable and

$$\frac{\partial \mathscr{R}}{\partial r^+}=0 \quad \text{at} \quad r^+=0. \tag{21b}$$

This latter condition holds, since it is easily seen from figures 1 and 2 that the concentration profile must be symmetric about $r^+=0$ along any one diameter.

Sets of eigenvalues α need to be calculated for each of the $\lambda = 1, 2, 3, \ldots$. The solution for $\mathscr{R}(r^+)\psi(x^+)$ for any one value of ω is thus

$$\mathscr{R}\psi=\sum_{n=1}^{n=\infty}K_n\mathscr{R}_n\exp\left[\frac{-2\alpha_n^2x^+}{R}\right], \tag{22}$$

where the coefficients K_n are determined from the initial profile. Thus at $x^+=0$ at any value of ω

$$\sum_{n=1}^{n=\infty}A_n\cos n\omega'=f(\omega)\sum_{n=1}^{n=\infty}K_n\mathscr{R}_n, \tag{23}$$

whilst

$$f(\omega)=\sum_{\lambda=1}^{\lambda=\infty}A'_\lambda\cos(\lambda\omega). \tag{24}$$

Thus,

$$K_n=\frac{\left[\dfrac{\cos n\omega'}{\sum_{\lambda=1}^{\lambda=\infty}A'_\lambda\cos(\lambda\omega)}\right]\displaystyle\int_0^{r_0^+}A_n\left(\frac{r}{r_0^+}\right)\mathscr{R}_nu^+r^+\,dr^+}{\displaystyle\int_0^{r_0^+}u^+r^+\mathscr{R}_n^2\,dr^+}, \tag{25}$$

and the concentration profile is given by

$$\theta=1+\sum^{n=\infty}C_n\phi_n\exp\left[\frac{-2\beta_n^2x^+}{R}\right]+\sum_{\lambda=1}^{\lambda=\infty}A'_\lambda\cos(\lambda\omega)\sum_{n=1}^{n=\infty}K_n\mathscr{R}_n\exp\left[\frac{-2\alpha_n^2x^+}{R}\right]. \tag{26}$$

(iv) *Description of the velocity profile and eddy diffusivities*

The velocity profile and radial eddy diffusivity of mass are assumed the same in the non-axisymmetric situation as in the axisymmetric situation. Accordingly, the descriptions established by Quarmby & Anand are used for these quantities.

A most useful result would be obtained if a simple relationship could be established between $\epsilon_{d,\omega}$ and $\epsilon_{d,r}$. Laufer (1954) and Sandborn (1955) have shown experimentally that near the centre of the tube conditions of isotropy prevail,

but that near the wall this is not so. It is reasonable to assume, as a start, that the ratio of $\epsilon_{d,\omega}$ to $\epsilon_{d,r}$ will be a function of radius, so that

$$\epsilon_{d,\omega} = F(r^+)\,\epsilon_{d,r}. \tag{27}$$

The evaluation of θ from (26) allows a comparison with experiment, from which the correctness of the assumption made concerning $F(r^+)$ may be established. In this work, we assume $F(r^+) = 1$, that is, that the radial and tangential eddy diffusivities of mass are equal at a point.

3. Calculations

Calculations were made of the eigenvalues α_n and constant K_n of (25) for the Reynolds numbers 20,800, 44,700, 81,900 and 119,000 for the discontinuous ring source, and Reynolds numbers 20,800 and 44,700 for the diametral line source. The eigenvalues β_n, and the values of the parameter r_0^+, are given for these Reynolds numbers in the results obtained for the symmetric situation in the first part of this work. The constants C_n, however, need recalculating to correspond with the symmetric part of the initial profile A_0, according to (8*b*).

The measured initial profiles at $x^+ = 0$ were described as functions of r and ω as follows. Fourier coefficients A_n were fitted to the experimental points for constant z. They were found by the method of Hildebrand (1955), using a technique due to Ralston & Wilf (1960). Polynomials in z, equation (5*b*), were then found for each A_n. The coefficient A'_λ was then found from (19). The constants K_n were evaluated for seven values of ω in the ranges 0 to $\frac{1}{2}\pi$ for the ring source and 0 to π for the line source. The tables of K_n, in particular, are very extensive, since there are accordingly seven values of K_n for each value of α_n.†

Use of the constants and eigenvalues obtained allows the non-dimensional concentration profile to be calculated from (26). This profile may be compared with experimental measurements to provide a test of the assumption that the tangential eddy diffusivity of mass is equal to the radial eddy diffusivity of mass.

4. Experimental investigations

(i) *Experimental apparatus*

The experimental apparatus is the same as that used by Quarmby & Anand in the first part of this work. The discontinuous ring source was made by covering part of the permeable surface of the continuous ring source with impermeable adhesive tape. The diametral line source consisted of a stainless steel hypodermic tube, of 0·0425 in. outside diameter, and of 0·030 in. inside diameter, in which a large number of small holes, of 0·010 in. diameter, were drilled. Nitrous oxide was fed in at both ends. The sources are shown in figures 1 and 2.

(ii) *Experimental measurements*

Measurements of the concentration profile were made at each traversing station for the Reynolds numbers listed above. For the discontinuous ring source,

† All the computed results for the eigenvalues and constants may be obtained from either author; they are too extensive to be given here.

extensive measurement was confined to $0 < \omega < \frac{1}{2}\pi$, and for the diametral line source, it was confined to $0 < \omega < \pi$. Measurements were also made over the rest of the cross-sectional area as a check. In all cases, consistent results were obtained.

5. Comparison between theory and experiment

Figures 3 and 4 show the development of the non-dimensional radial concentration profile between $x^+ = 0$ and $x^+ = 92{\cdot}95$, for the discontinuous ring source for $R = 20{,}800$ and $R = 119{,}000$, with $\omega = 0$ and $\omega = \frac{1}{4}\pi$. Figure 5 shows the

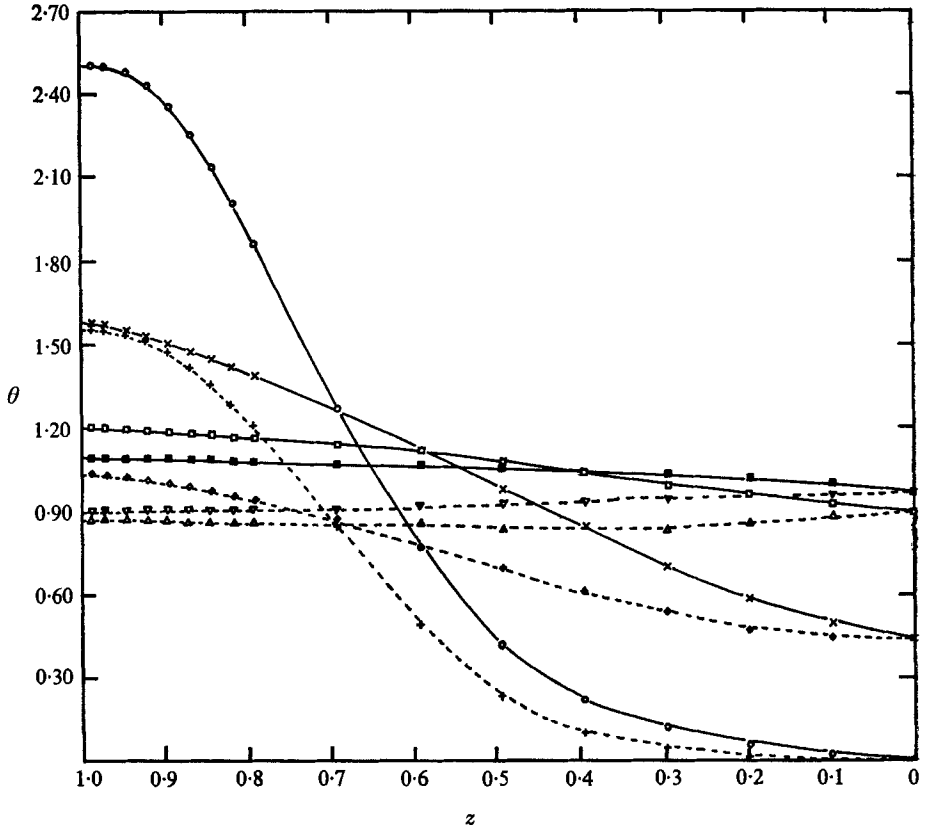

FIGURE 3. Radial concentration profiles for ring source, $R = 20{,}800$, $\omega = 0$ and 1·5714 rad: theory, equation (26), ——; experiment, x^+: ○, 0·00; ×, 18·60; □, 51·66; ■, 92·98. $\omega = 0{\cdot}7857$ rad: theory, equation (26), – – —; experiment, x^+: +, 0·00; ▽, 18·60; ◇, 51·66; △, 92·98.

axial development for $R = 20{,}800$ at $\omega = \frac{1}{4}\pi$, for various values of z. It may be noted that, for large x^+, the measured values of θ approached unity. The developing radial profile for the diametral line source is shown in figure 6 for $R = 20{,}800$ for $\omega = 0$, and in figure 7 for $\omega = \frac{1}{2}\pi$. The axial development for $\omega = \frac{1}{2}\pi$ is shown in figure 8 for various values of z. In each of these results, the agreement between theory and experiment is most satisfactory.

Direct measurement of the tangential eddy diffusivity of mass was made from the concentration profiles. From (2),

$$u^+r_0^+\frac{\partial\theta}{\partial x^+}=\frac{1}{z}\frac{\partial}{\partial z}\left[z\left(\frac{1}{S}+\frac{\epsilon_{d,r}}{\nu}\right)\frac{\partial\theta}{\partial z}\right]+\frac{1}{z^2}\frac{\partial}{\partial\omega}\left[\left(\frac{1}{S}+\frac{\epsilon_{d,\omega}}{\nu}\right)\frac{\partial\theta}{\partial\omega}\right]; \tag{28}$$

and, since $\epsilon_{d,\omega}$ is not a function of ω,

$$\frac{\epsilon_{d,\omega}}{\nu}=\frac{u^+r_0^+z^2\dfrac{\partial\theta}{\partial x^+}-z\dfrac{\partial}{\partial z}\left[z\left(\dfrac{1}{S}+\dfrac{\epsilon_{d,r}}{\nu}\right)\dfrac{\partial\theta}{\partial z}\right]}{\dfrac{\partial^2\theta}{\partial\omega^2}}-\frac{1}{S}. \tag{29}$$

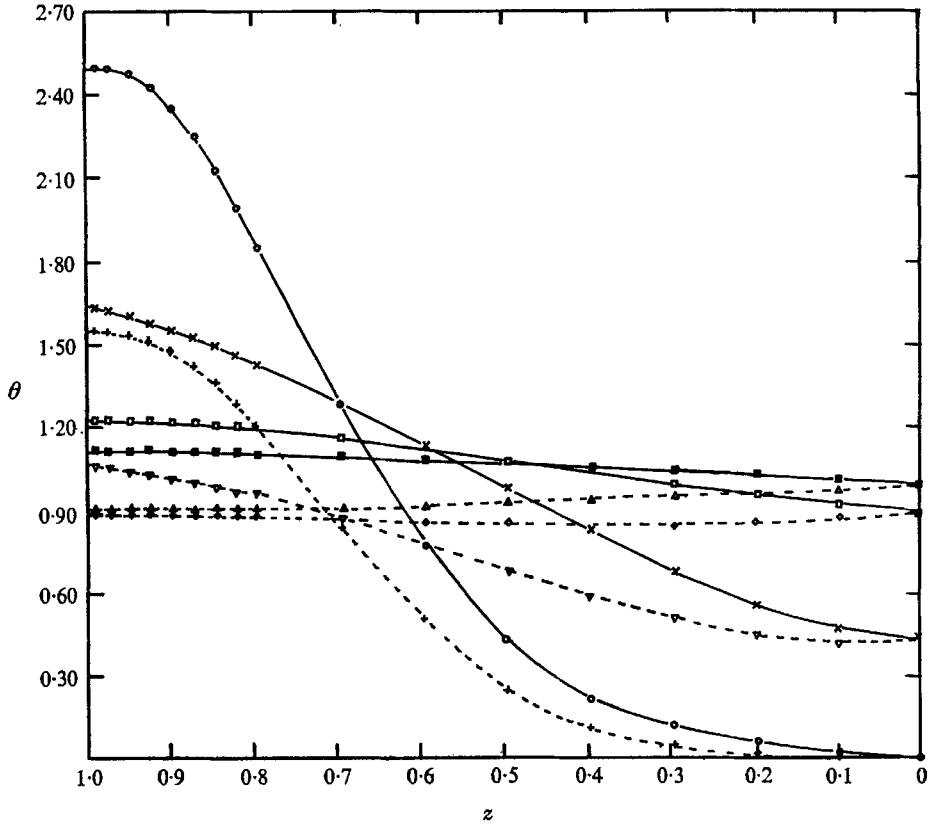

FIGURE 4. Radial concentration profiles for ring source, R = 119,000. ω = 0 and 1·5714 rad: theory, equation (26), ——; experiment, x^+: ○, 0·00; ×, 81·60; □, 51·66; ■, 92·98. ω = 0·7857 rad: theory, equation (26), – – – –; experiment, x^+: +, 0·00; ▽, 18·60; ◇, 51·66; △, 92·98.

The numerical evaluation of (29) used the same techniques as were used in the first part of this work to calculate $\epsilon_{d,r}$. The value of $\epsilon_{d,r}$ in (29) was also taken from the results of the first part. Since $\epsilon_{d,r}$ is not a function of ω, we should get the same result at whatever value of ω it is calculated. However, the numerical evaluation of second derivatives is a dubious process. Figure 9 shows the tangential

concentration profiles at $x^+ = 31{\cdot}0$, from which $\partial^2\theta/\partial\omega^2$ was evaluated for $R = 20{,}800$. It is clear that, considering the limitations of the method, meaningful results for $\partial^2\theta/\partial\omega^2$ could be expected only at $\frac{1}{8}\pi$, where $\partial\theta/\partial\omega$ is greatest.

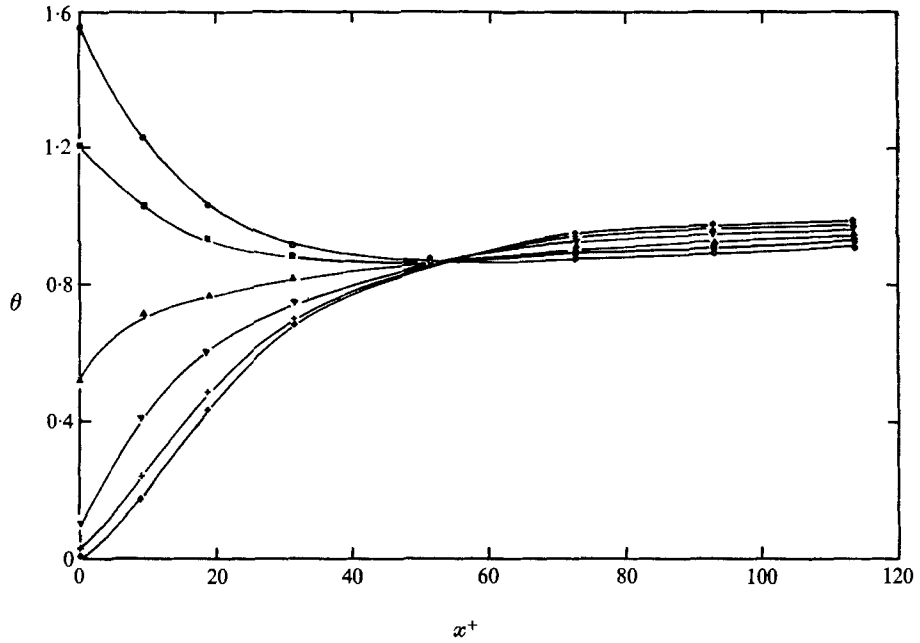

FIGURE 5. Axial development of concentration profile for ring source, $R = 20{,}800$, $\omega = 0{\cdot}7857$ rad: theory, equation (26), ——; experiment, z: ○, 0·990; ■, 0·793; △, 0·594; ▽, 0·396; +, 0·198; ◇, 0·000.

Figure 10 compares the measured values of $\epsilon_{d,\omega}$ with the theoretical expression given by assuming $F(r^+) = 1$ and use of the expression for the radial eddy diffusivity developed in the first part of this work. The agreement is quite satisfactory. This result may also be compared with Jenkins' (1951) expression for the ratios of the eddy diffusivity of mass to that of momentum. For non-axisymmetric mass transfer Jenkins' expression, which relates the radial eddy diffusivities of heat and momentum, is modified to become

$$\frac{\epsilon_{d,\omega}}{\epsilon_{m,r}} = Sc\,\frac{1-\dfrac{90}{\pi^6}\dfrac{lv}{D}\displaystyle\sum_{n=1}^{n=6}\frac{1}{n^6}\left[1-\exp\left(\frac{-n^2\pi^2 D}{lv}\right)\right]}{1-\dfrac{90}{\pi^6}\dfrac{lv}{\nu}\displaystyle\sum_{n=1}^{n=6}\frac{1}{n^6}\left[1-\exp\left(\frac{-n^2\pi^2\nu}{lv}\right)\right]}, \tag{30}$$

where l is the mixing length and v the supposed velocity of the spherical turbulent eddy. The comparison with the present results is shown in figure 11.

The good agreement between theory and experiment seems to establish that the radial and tangential eddy diffusivities of mass are equal at any point in a fully developed turbulent flow. However, it may be that the solution of (1) is not too sensitive to the magnitude and shape of $F(r^+)$. In axisymmetric cases, quite good agreement has been achieved between experiment and theories, which

differed markedly from each other. A notable example is the prediction of the turbulent velocity profile in a plain tube. The present result is based on a difficult set of measurements. It might well be that these do no more than *fail to disprove* the hypothesis that, in general, $\epsilon_{d,\omega}$ and $\epsilon_{d,r}$ are equal. It is apparently valid in

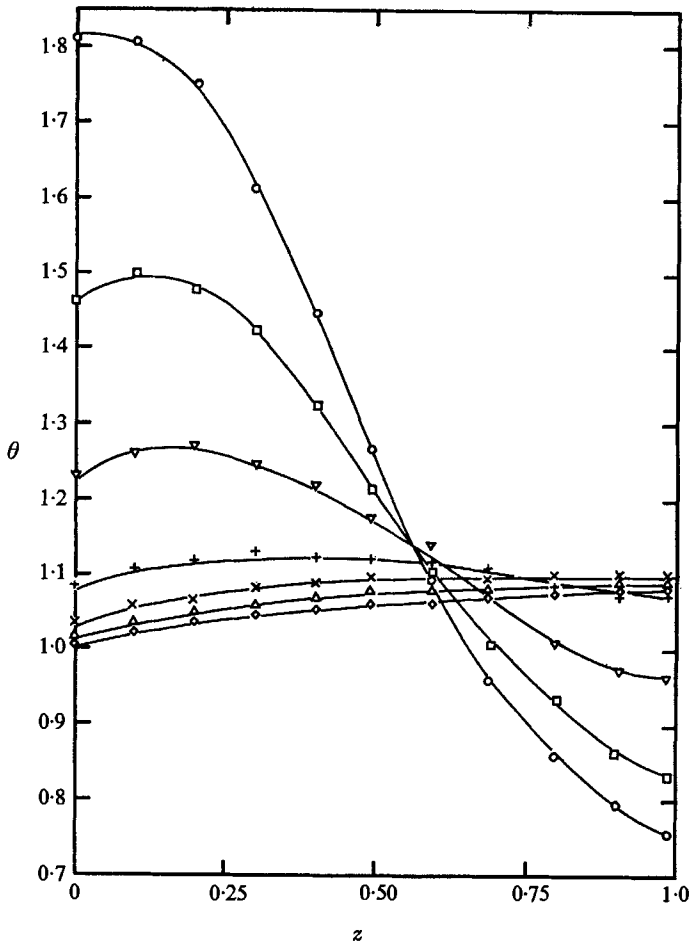

FIGURE 6. Radial concentration for line source, R = 20,800, ω = 0 rad: theory, equation (26), ——; experiment, x^+: ○, 0·00; □, 9·30; ▽, 21·70; +, 42·36; ×, 63·02; △, 83·68; ◇, 104·34.

the present case, but its validity must be established for other cases, especially for fluids of high Prandtl number, before it becomes unchallengeable.

The apparent equivalence of $\epsilon_{d,r}$ and $\epsilon_{d,\omega}$ found here has some significance, when its relevance to the mixing length theory is considered. The time mean rate of mass transfer in the radial and tangential directions may be written:

$$J_{d,r} = \rho \overline{V|c(r_1) - c(r_2)|}, \tag{31a}$$

and

$$J_{d,\omega} = \rho \overline{W|c(s_1) - c(s_2)|}, \tag{31b}$$

where s is the arc length.

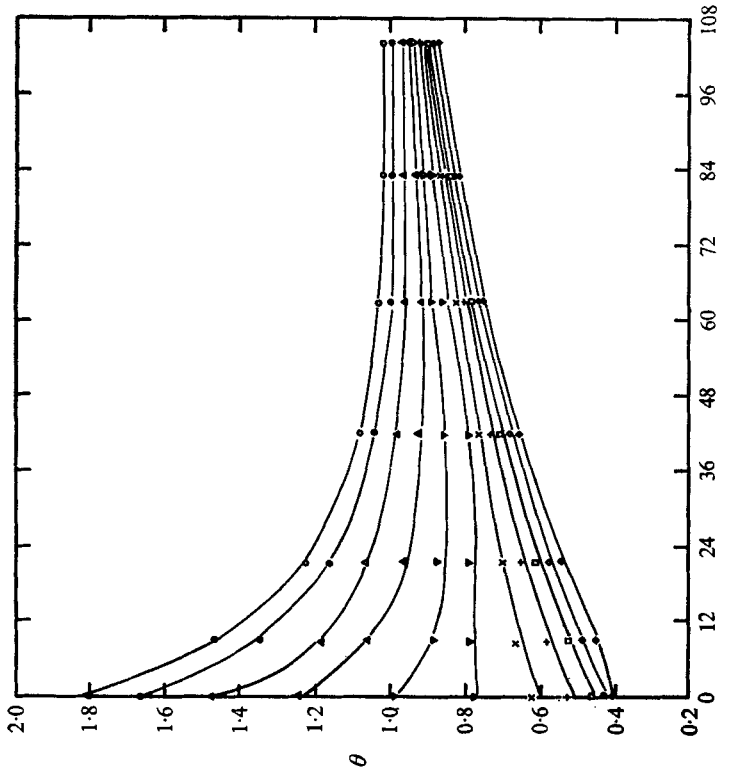

FIGURE 8. Axial development of concentration profile for line source, $R = 20{,}800$, $\omega = 1.5714$ rad: theory, equation (26), ——; experiment, z: ○, 0·990; ●, 0·891; △, 0·792; ▲, 0·693; ▽, 0·594; ▼, 0·495; ×, 0·396; +, 0·297; □, 0·198; ◇, 0·099; ◆, 0·000.

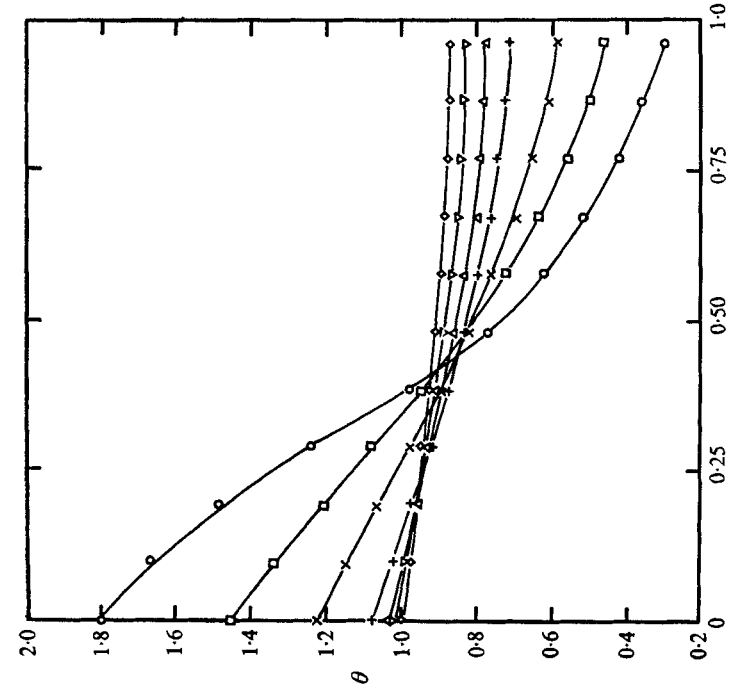

FIGURE 7. Radial concentration for line source, $R = 20{,}800$, $\omega = 1.5714$ rad: theory, equation (26), ——; experiment, x^+: ○, 0·00; □, 9·30; ×, 21·70; +, 42·36; △, 63·02; ▽, 83·68; ◇, 104·34.

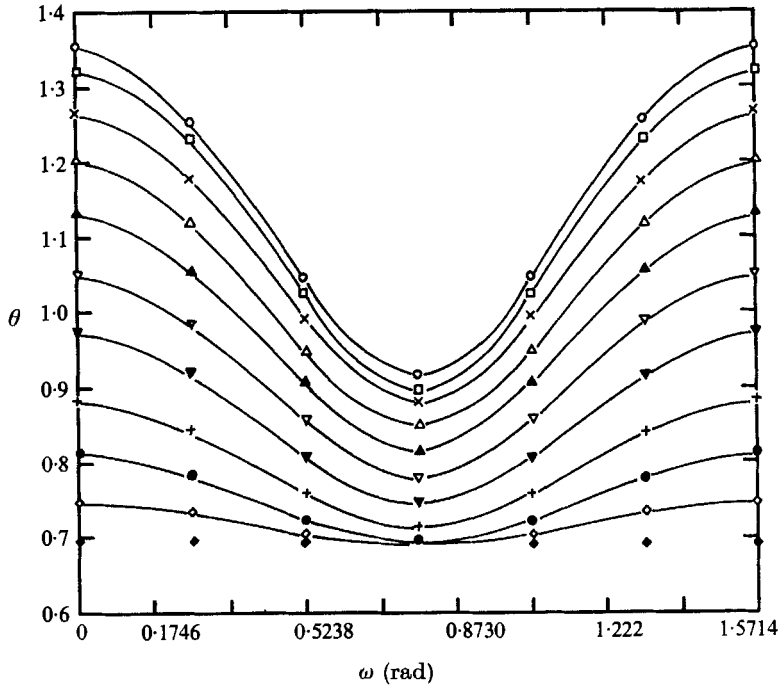

FIGURE 9. Tangential variation of concentration profile for ring source at $x^+ = 31$. $R = 20{,}800$. Theory, equation (26), ——; experiment, z: ○, 0·990; □, 0·897; ×, 0·793; △, 0·693; ▲, 0·594; ▽, 0·495; ▼, 0·396; +, 0·297; ●, 0·198; ◇, 0·099; ◆, 0·000.

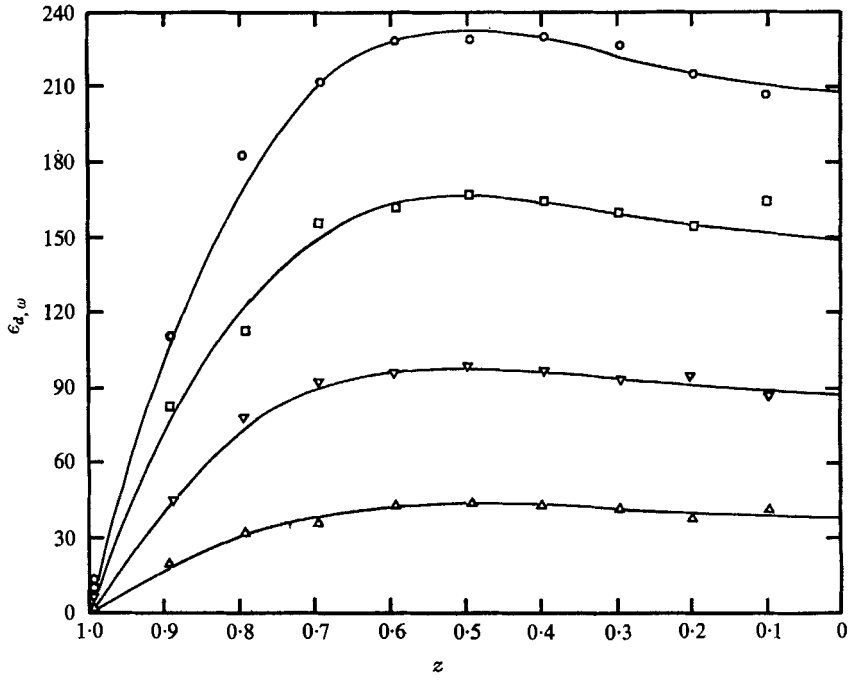

FIGURE 10. Tangential eddy diffusivity of mass. Theory, equation (30), ——; experiment: ○, $R = 119{,}100$; □, 81,950; ▽, 44,700; △, 20,800.

Following Goldstein (1938, p. 205), using the expansion in a Taylor series of equations (31*a*) and (31*b*) and introducing the mixing lengths $l_{d,r}$ and $l_{d,\omega}$, we may write

$$J_{d,r} = -\rho l_{d,r} \overline{v}' \frac{dc}{dr} = -\rho \epsilon_{d,r} \frac{dc}{dr}, \tag{32a}$$

where $\overline{v}'$ and $\overline{w}'$ are time averages of the velocity fluctuations in r and s, and

$$J_{d,\omega} = -\rho l_{d,\omega} \overline{w}' \frac{dc}{ds} = -\epsilon_{d,\omega} \frac{dc}{ds}. \tag{32b}$$

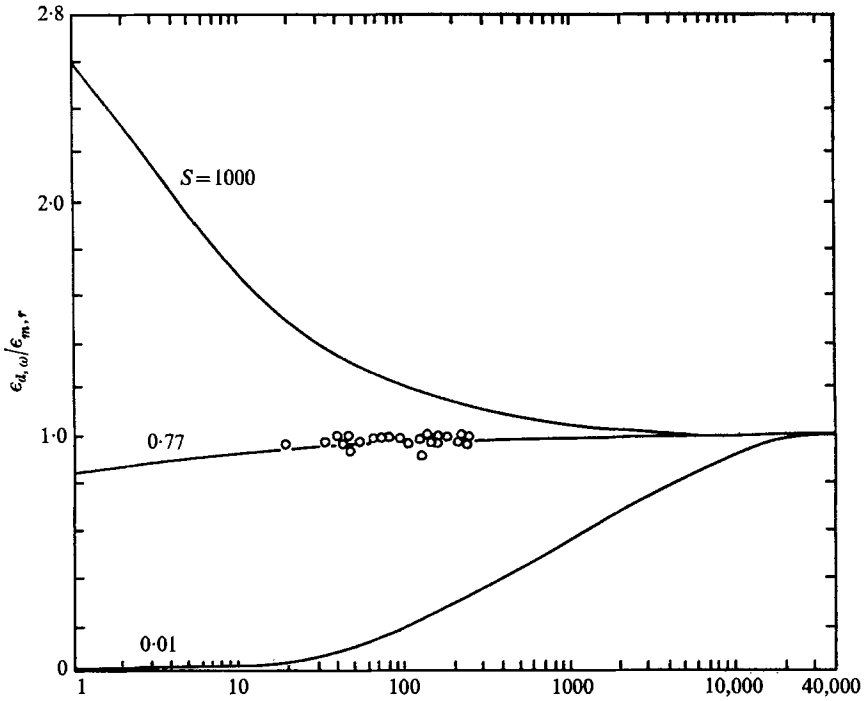

FIGURE 11. Ratio of tangential eddy diffusivity of mass to radial eddy diffusivity of momentum. ——, Jenkins' theory, equation (30); O, experimental measurements.

That is
$$\epsilon_{d,r} = -l_{d,r} \overline{v}', \tag{33a}$$

and
$$\epsilon_{d,\omega} = -l_{d,\omega} \overline{w}'. \tag{33b}$$

Since the present results indicate that $\epsilon_{d,r}$ and $\epsilon_{d,\omega}$ are equal, we may conclude that

$$\frac{l'_{d,r}}{l'_{d,\omega}} = \frac{\overline{w}'}{\overline{v}'}. \tag{34}$$

The experiments of Laufer (1954) and Sandborn (1955) show that near the wall $\overline{v}'$ and $\overline{w}'$ are not equal. Accordingly, the present results suggest that the mixing lengths in the radial and tangential directions are not equal near the wall. On the other hand, Laufer and Sandborn found $\overline{v}'$ and $\overline{w}'$ to be equal at the centre of the tube. Thus, we may conclude that in the centre the mixing lengths, also, are equal.

6. Conclusion

The analysis presented for mass transfer, into a fully developed turbulent flow in a plain tube in a non-axisymmetric situation, is in good agreement with experiments for $20{,}000 < R < 120{,}000$. The results are equally good, whether the mass transfer is mainly taking place in the central core of the flow, or in the wall region. The good agreement between theory and experiment suggests the correctness of the assumption made in the analysis, that the tangential and radial eddy diffusivities of mass are equal. Further investigation with fluids of Prandtl number greater than unity should provide a more stringent test of this assumption.

As a consequence of the apparent equivalence of the radial and tangential eddy diffusivities of mass at a point, it is suggested that the mixing lengths, in the radial and tangential directions, are related by

$$\frac{l_{d,r}}{l_{d,\omega}} = \frac{\overline{w'}}{\overline{v'}}.$$

Thus, at the centre of the tube, the mixing lengths are equal but, near the wall of the tube, they are not equal.

The present results for mass transfer are considered very relevant to heat transfer in non-axisymmetric situations, especially for gases.

REFERENCES

GOLDSTEIN, S. 1938 *Modern Developments in Fluid Mechanics*, vol. 1. Oxford University Press.

HALL, W. B. & HASHIMI, J. A. 1964 *Proc. Instn mech. Engrs*, **178**, 1.

HANOLD, R. 1967 *Trans. Am. Soc. mech. Engrs*, C **89**, 268.

HILDEBRANDT, F. B. 1955 *Numercial Analysis*. New York: McGraw Hill.

JENKINS, R. 1951 *Proc. Heat Transfer and Fluid Mechanics Inst.* p. 147. Stanford, California.

LAUFER, J. 1954 The structure of turbulence in fully developed pipe flow. *NACA* Rep. no. 1174.

QUARMBY, A. & ANAND, R. K. 1969 *J. Fluid Mech.* **38**, 433.

RALSTON, A. & WILF, H. S. 1960 *Mathematical Models for Digital Computers*. New York: Wiley.

REYNOLDS, W. C. 1963 *Int. J. Heat Mass Transfer*, **6**, 445.

SANDBORN, J. A. 1955 Experimental evaluation of momentum terms in turbulent pipe flow. *NACA* TN 3266.

SPARROW, E. M. & BLACK, A. W. 1967 *Trans. Am. Soc. mech. Engrs*, C **89**, 258.

SPARROW, E. M. & LIN, S. H. 1963 *Int. J. Heat Mass Transfer*, **6**, 866.